$2CH_3CN\subset(n\text{-}Bu_4N)_2[\{Ir(1,5\text{-}COD)\}_6W_4O_{16}]\cdot 2CH_3CN$: A Hybrid Inorganic−Organometallic, Flexible Cavity Host, Acetonitrile−Guest Complex Composed of a $[W_4O_4]^{n+}$ Tetratungstate Cube and Six Polyoxoanion-Supported (1,5-COD)Ir^+ Organometallic Groups

Yoshihito Hayashi, Frank Müller, Yin Lin, Susie M. Miller, Oren P. Anderson, and Richard G. Finke*

Contribution from the Department of Chemistry, Colorado State University, Fort Collins, Colorado 80523

Received January 31, 1997. Revised Manuscript Received September 3, 1997[⊗]

Abstract: The tetratungstate polyoxoanion-supported organometallic compound $2CH_3CN\subset(n\text{-}Bu_4N)_2[\{Ir(1,5\text{-}COD)\}_6W_4O_{16}]\cdot 2CH_3CN$ ($2CH_3CN\subset$**1**$\cdot 2CH_3CN$) is reported, a complex which exhibits an unusual "methyl-first" CH_3CN inclusion ("$\subset$") chemistry. The synthesis of $2CH_3CN\subset$**1**$\cdot 2CH_3CN$ was accomplished by the reaction of 3 equiv of $[Ir(1,5\text{-}COD)Cl]_2$ with 4 equiv of $(n\text{-}Bu_4N)_2WO_4$; an X-ray diffraction single-crystal structure shows that the four tungsten atoms in of $2CH_3CN\subset$**1**$\cdot 2CH_3CN$ are located in tetrahedral positions and combine with four bridging oxygens to yield a tungsten-oxygen cubane structure. The cubane core tungsten atoms are capped by six surrounding $[Ir(1,5\text{-}COD)]^+$ groups in an octahedral arrangement relative to the cube, with each $[Ir(1,5\text{-}COD)]^+$ group coordinated by two terminal oxygen atoms from the tetratungstate unit. Two sets of flexible acetonitrile-binding cavities, formed between each three of the six $[Ir(1,5\text{-}COD)]^+$ groups, form a roughly tetrahedral array surrounding the cube. This host-guest complex binds acetonitrile methyl-first, that is, with the methyl group rather than the nitrile group oriented toward a cubane core oxygen atom. The $C_{Me}\cdots O$ nonbonded distances fall in the range 3.10−4.46 Å for $C_{Me}\cdots(\mu_2\text{-}O)$ and 3.08−4.02 Å for $C_{Me}\cdots(\mu_3\text{-}O)$. Acetonitrile-free **1** was also prepared, and its possible acetonitrile and toluene complexation in benzene and methylene chloride solution was studied by NMR. No binding between acetonitrile or toluene and **1** in solution is observed, even when using greater than 300 mol equiv of guest relative to **1**. Therefore, the host-guest interaction between **1** and acetonitrile appears to be weak ($K_{eq} < 10\ M^{-1}$), possibly being limited to the solid state.

Introduction

Polyoxoanion-supported organometallic compounds[1,2] are of interest for their novel compositions, their structures, and their ability to serve as discrete analogues[3] of solid-oxide-supported heterogeneous catalysts or as precursors to new types of homogeneous catalysts.[4,5] Despite the well-known structural chemistry of polyoxometalates,[6,2a] the number of different structural types is relatively small, confined historically primarily to the Keggin (e.g., $PW_{12}O_{40}^{3-}$), Wells−Dawson (e.g., $P_2W_{18}O_{62}^{6-}$), and Lindquist hexametalate (e.g., $W_6O_{19}^{2-}$) core structures.[6]

Much less studied but of fundamental interest is the metal-oxygen cubane core, for example, $[W_4O_4]^{n+}$. Indeed, and although the chemistry of sulfur-containing transition complexes with a cubane core is well developed,[7] fewer of the corresponding metal-oxygen cubane core complexes are known.[8−10] Metal-oxygen cubane cores containing *hydroxide* ligands, for example, $[(OC)_3W(\mu_3\text{-}OH)_4]_4^{4-}$,[8b,i] have been observed as a hydrolysis product of organometallic compounds. More recently, middle-to-late transition metal-oxygen cubane-core complexes[9] have been studied as bioinorganic models for the Mn_4O_4-dependent, photosynthetic water oxidation center in green plants.[10,11] In addition, a $Mo_4O_4^{6+}$ core is also observed as a building block in extended solids.[12] However, a discrete, structurally well-characterized $[W_4(\mu_3\text{-}O)_4]^{n+}$ core has not been previously reported.

The inclusion of neutral molecules such as hydrocarbons[13] by inorganic[14,15] and more recently organometallic complexes, specifically $[\{Ru(\eta^6\text{-arene})\}_3(CTV)]^{6+}$ or $[\{Ir(\eta^5\text{-}Cp^*)\}_3(CTV)]^{6+}$

* Corresponding author: e-mail, Rfinke@lamar.colostate.edu; FAX, (970)-491-1801.

⊗ Abstract published in *Advance ACS Abstracts*, October 15, 1997.

(1) Day, V. W.; Klemperer, W. G. *Science* **1985**, *228*, 533−541. See also the list of references (6 and 7a−j) provided in ref 2b listed below.

(2) (a) A short review: Finke, R. G. In *Polyoxometalates: From Platonic Solids to Anti-Retroviral Activity*; Proceedings of the July 15−17, 1992 Meeting at the Center for Interdisciplinary Research in Bielefeld, Germany; Müller, A., Pope, M. T., Eds.; Kluwer Academic Publishers: Dordrecht, The Netherlands, 1992; pp 267−280. (b) Pohl, M.; Lyon, D. K.; Mizuno, N.; Nomiya, K.; Finke, R. G. *Inorg. Chem.* **1995**, *34*, 1413−1429. (c) See also the list of references (8a−l and 9a−i) provided elsewhere.[2b]

(3) See footnote 5 elsewhere[2b] for a list of 30 references to other discrete, but nonpolyoxometalate, "oxo-type" homogeneous ligand systems that have been investigated as soluble analogues of solid-oxide-supported catalysts.

(4) Oxidations using O_2: (a) Mizuno, M.; Lyon, D. K.; Finke, R. G. *J. Catal.* **1991**, *128*, 84. (b) Mizuno, M.; Lyon, D. K.; Finke, R. G. U.S. Patent 5,250,739, issued October 5, 1993. (c) Mizuno, N.; Weiner, H.; Finke, R. G. *J. Mol. Catal. A: Chem.* **1996**, *114*, 15.

(5) Catalytic hydrogenation studies, including the discovery of novel polyoxoanion- and Bu_4N^+-stabilized, isolable $Ir(0)_{\sim 300}$ nanocluster catalysts: Lin, Y.; Finke, R. G. *J. Am. Chem. Soc.* **1994**, *116*, 8335−8353. Lin, Y.; Finke, R. G. *Inorg. Chem.* **1994**, *33*, 4891−4910. Edlund, D. J.; Finke, R. G.; Saxton, R. J. U.S. Patent 5,116,796, issued May 29, 1992. A review: Aiken J. D., III; Lin, Y.; Finke, R. G. *J. Mol. Catal. A: Chem.* **1996**, *114*, 29−51. Watzky, M. A.; Finke, R. G. *J. Am. Chem. Soc.* **1997**, *119*, 10382−10400.

(6) (a) Pope, M. T. *Heteropoly and Isopoly Oxometalates*; Springer-Verlag: New York, 1983. (b) Pope, M. T.; Müller, A. *Angew. Chem., Int. Engl. Ed.* **1991**, *30*, 34−48.

S0002-7863(97)00336-3 CCC: $14.00

(where arene = 4-MeC$_6$H$_4$CHMe$_2$, CTV = 2,3,7,8,12,13-hexamethoxy-5,10-dihydro-15*H*-tribenzo[*a*,*d*,*g*]cyclononene),[16] is another area of current interest. The inclusion of acetonitrile, of particular relevance to the present studies, has been observed in molecular, purely *inorganic* complexes, specifically dodecavanadate,[17] [$CH_3CN\subset(V_{12}O_{32}^{4-})$], and also a polyvanadate[15] [$2CH_3CN\subset(V_{14}O_{22}(OH)_4(PhPO_3)_8)^{6-}$]. Efforts to introduce organometallic groups into macrocyclic inclusion hosts such as calix[4]arene[18] have also appeared with the overall goal of developing shape-selective catalytic reactions operating via binding- plus active-site "synergetic effects".[18]

Herein we report the discovery[19] and then the rational synthesis and crystallographic structure determination of $2CH_3CN\subset(n\text{-}Bu_4N)_2[\{Ir(1,5\text{-}COD)\}_6W_4O_{16}]\cdot 2CH_3CN$, hereafter $2CH_3CN\subset\mathbf{1}\cdot 2CH_3CN$ (1,5-COD = 1,5-cyclooctadiene), as well as NMR studies of the acetonitrile-free complex **1**. This unusual type of *hybrid inorganic−organometallic host complex* contains a $[W_4O_4]^{16+}$ cubane core within a $[W_4O_{16}]^{8-}$ polyoxoanion, which is in turn surrounded by six $[Ir^{I}(1,5\text{-COD})]^+$ groups. The $[Ir^{I}(1,5\text{-COD})]^+$ groups form flexible and novel composition cavities which bind two CH_3CN groups in the solid-state in a little precedented methyl- rather than nitrile-first fashion. Such *molecular* inorganic/organometallic hosts for *uncharged* ligands such as hydrocarbons[13] are not common[17] and, thus, of fundamental interest for comparison to the better-known area of inclusion complexes of inorganics.[14]

Results and Discussion

Synthesis. The title compound $2CH_3CN\subset\mathbf{1}\cdot 2CH_3CN$ (also abbreviated "Ir_6W_4") was synthesized[19] from the reaction of 3 equiv of $[Ir(1,5\text{-COD})Cl]_2$ and 4 equiv of $(n\text{-}Bu_4N)_2WO_4$ in acetonitrile under a nitrogen atmosphere according to the Experimental Procedure provided. It was formed in good yields using the above molar ratio, but even ratios such as 1:1 provide the Ir_6W_4 complex, indicating that it is at least the kinetically, and probably also the thermodynamically, preferred product. The resultant light-yellow crystals were characterized by elemental analysis, FAB mass spectrometry, IR spectroscopy, and single-crystal X-ray diffraction (vide infra). The presence of 4.0 (±0.4) molecules of acetonitrile per polyoxotungstate anion was confirmed by ^{1}H NMR on a sample of X-ray-quality crystals dissolved in $CDCl_3$, in quantitative agreement with the crystallographically determined formula $2CH_3CN\subset\mathbf{1}\cdot 2CH_3CN$. Two of the acetonitrile molecules are easily lost, and the remaining two acetonitrile molecules can be removed by heating $2CH_3CN\subset\mathbf{1}\cdot 2CH_3CN$ under vacuum overnight to give acetonitrile-free **1**. The IR spectrum of **1** exhibited a strong, diagnostic band at 835 cm^{-1} in the region characteristic of ν(M−O) stretching vibrations (M = W, Ir). The FAB mass spectrum of $2CH_3CN\subset\mathbf{1}\cdot 2CH_3CN$ exhibited the appropriate molecular ion peak at *m*/*z* 3278 as well as a peak at *m*/*z* 3038 [M − (*n*-Bu$_4$N) + 2H]$^+$. In addition, the calculated isotropic distribution patterns matched those expected for the naturally occurring isotopes of the relevant atoms (see the Supporting Information).

Structure. The X-ray diffraction study of $2CH_3CN\subset\mathbf{1}\cdot 2CH_3CN$ reveals two crystallographically independent formula units of **1** in the asymmetric unit; these two formula units exhibit very similar structures (see Figure 1 for the structure of the anion of **1a**). The anion in **1** consists of a tungstate tetramer, $[W_4O_{16}]^{8-}$, capped by six $[Ir(1,5\text{-COD})]^+$ organometallic groups each bound to two cisoid terminal oxygen atoms over a face of the distorted-cubic core. The four tungsten atoms are arranged in a tetrahedron, and the six iridium atoms are arranged in an octahedron about the center of the W_4O_4 "cube", providing the first example of the tetratungstate or $[W_4O_4]^{n+}$ cube structure in a discrete complex. Each $[W_4O_{16}]^{8-}$ unit contains three

(7) (a) Holm, R. H.; Ciurli, S.; Weigd, J. A. *Prog. Inorg. Chem.* **1990**, *38*, 1−74. (b) Holm, R. H. *Adv. Inorg. Chem.* **1992**, *38*, 1−71.

(8) (a) Albano, V.; Bellon, P.; Ciani, G.; Manassero, M. *J. Chem. Soc., Chem. Commun.* **1969**, 1242−1243. (b) Albano, V. G.; Ciani, G.; Manassero, M.; Sansoni, M. *J. Organomet. Chem.* **1972**, *34*, 353−365. (c) Bottomley, F.; Paez, D. E.; White, P. S. *J. Am. Chem. Soc.* **1981**, *103*, 5581−5582. (d) Bottomley, F.; Paez, D. E.; White, P. S. *J. Am. Chem. Soc.* **1982**, *104*, 5651−5657. (e) Bottomley, F.; Paez, D. E.; Sutin, L.; White, P. S.; Köhler, F. H.; Thompson, R. C.; Westwood, N. P. C. *Organometallics* **1990**, *9*, 2443−2454. (f) Bottomley, F.; Chen, J.; MacIntosh, S. M.; Thompson, R. C. *Organometallics* **1991**, *10*, 906−912. (g) Johnson, B. F. G.; Lewis, Y.; Williams, I. G.; Wilson, Y. *J. Chem. Soc., Chem. Commun.* **1966**, 391. (h) Bright, D. *J. Chem. Soc., Chem. Commun.* **1970**, 1169. (i) Hayashi, Y.; Toriumi, K.; Isobe, K. *J. Am. Chem. Soc.* **1988**, *110*, 3666−3668. (j) Lin, J. T.; Yeh, S. K.; Lee, G. H.; Wang, Y. *J. Organomet. Chem.* **1989**, *361*, 89−99. (k) McNeese, T. J.; Cohen, M. B.; Foxman, B. M. *Organometallics* **1984**, *3*, 552−556. (l) Nuber, B.; Oberdorfer, F.; Ziegler, M. L. *Acta Crystallogr., Sect. B.* **1981**, *B37*, 2062−2064. (m) Preston, H. S.; Mills, J. C.; Kennard, C. H. L. *J. Organomet. Chem.* **1968**, *14*, 447−452.

(9) (a) McKee, V.; Shepard, W. B. *J. Chem. Soc., Chem. Commun.* **1985**, 158−159. (b) Brooker, S.; McKee, V.; Shepard, W. B.; Pannell, L. K. *J. Chem. Soc., Dalton Trans.* **1987**, 2555−2562. (c) Dedert, P. L.; Sorrell, T.; Marks, T. J.; Ibers, J. A. *Inorg. Chem.* **1982**, *21*, 3506−3517. (d) Dimitrou, K.; Folting, K.; Streib, W. E.; Christou, G. *J. Am. Chem. Soc.* **1993**, *115*, 6432−6433. (e) Halcrow, M. A.; Sun, J.-S.; Huffman, J. C.; Christou, G. *Inorg. Chem.* **1995**, *34*, 4167−4177. (f) Pence, L. E.; Caneschi, A.; Lippard, S. J. *Inorg. Chem.* **1996**, *35*, 3069−3072. (g) Shoner, S. C.; Power, P. P. *Inorg. Chem.* **1992**, *31*, 1001−1010. (h) Taft, K. L.; Caneschi, A.; Pence, L. E.; Deifs, C. D.; Papaefthymiou, G. C.; Lippard, S. J. *J. Am. Chem. Soc.* **1993**, *115*, 11753−11766.

(10) (a) Christou, G. *Acc. Chem. Res* **1989**, *22*, 328. (b) Brudvig, G. W.; Crabtree, R. H. *Proc. Natl. Acad. Sci. U.S.A.* **1986**, *83*, 4586. (c) Brudvig, G. W.; Thorp, H. H.; Crabtree, R. H. *Acc. Chem. Res* **1991**, *24*, 311.

(11) EXAFS data of photosystem II show, however, that its Mn_4O_4 core is less symmetric than the isolated Mn_4O_4 cubane models: Wieghardt, K. *Angew. Chem., Int. Ed. Engl.* **1994**, *33*, 725−728.

(12) (a) Haushalter, R. C. *J. Chem. Soc., Chem. Commun.* **1987**, 1566−1568. (b) Lii, K. H.; Haushalter, R. C.; O'Connor, C. J. *Angew. Chem., Int. Ed. Engl.* **1987**, *26*, 549−551.

(13) For hydrocarbon inclusion or encapsulation complexes based on *organic* hosts, see: (a) Branda, N.; Wyler, R.; Rebek, J., Jr. *Science* **1994**, *263*, 1267−1268. (b) Meissner, R. S.; Mendoza, J.; Rebek, J., Jr. *Science* **1995**, *270*, 1485−1488.

(14) For a review of both solid-state and molecular inorganic inclusion and encapsulation complexes, see: Müller, A.; Reuter, H.; Dillinger, S. *Angew. Chem., Int. Ed. Engl.* **1995**, *34*, 2328−2361 and references therein.

(15) Khan, M. I.; Zubieta, J. *Angew. Chem., Int. Ed. Engl.* **1994**, *33*, 760−762.

(16) [{Ru(η^6-arene)}$_3$(CTV)]$^{6+}$ or [{Ir(η^5-Cp*)}$_3$(CTV)]$^{6+}$ employ up to three surrounding organometallic groups to create cavities which form inclusion complexes with both neutral molecules and monoanions such as BF_4^-: Holman, K. T.; Halihan, M. M.; Jurisson, S. S.; Atwood, J. L.; Burkhalter, R. S.; Mitchell, A. R.; Steed, J. W. *J. Am. Chem. Soc.* **1996**, *118*, 9567−9576.

(17) (a) Day, V. W.; Klemperer, W. G.; Yaghi, O. M. *J. Am. Chem. Soc.* **1989**, *111*, 5959−5961. (b) Klemperer, W. G.; Marquart, T. A.; Yaghi, O. M. *Mater. Chem. Phys.* **1991**, *29*, 97−104. (c) The Day−Klemperer−Yaghi complex has attracted computational interest: Rohmer, M.-M.; Devémy, J.; Wiest, R.; Bénard, M. *J. Am. Chem. Soc.* **1996**, *118*, 13007−13014.

(18) Loeber, C.; Matt, D.; Briard, P.; Grandjean, D. *J. Chem. Soc., Dalton Trans.* **1996**, 513−524.

(19) (a) The original synthesis and discovery of **1** was serendipitous and as follows: In a drybox under N_2, $(n\text{-}Bu_4N)_7[SiW_9Nb_3O_{40}]$[19b] (1 g, 0.352 mmol) and [(1,5-COD)Ir(CH$_3$CN)$_2$](BF$_4$) (165 mg, 1 equiv) were placed in CH_3CN and stirred for 20 min, the mixture was then evaporated to dryness under vacuum, and the resultant solid was redissolved in 2.5 mL of CD_3CN and placed inside a J. Young NMR tube. Next, ^{183}W NMR experiments were performed from 20 to 60 °C with the intent of better understanding the NMR properties of $[(1,5\text{-COD})Ir\cdot SiW_9Nb_3O_{40}]$.[19b] After the NMR experiments, the NMR tube was returned to the drybox to stand in hope of growing X-ray diffraction quality single crystals of $[(1,5\text{-COD})Ir\cdot SiW_9Nb_3O_{40}]$. After storage in the drybox for 1 year, pale-yellow single crystals were noticed and, hence, were collected from the viscous solution. A preliminary single-crystal X-ray diffraction structural analysis revealed the unexpected structure shown for **1**. We suspect, but have not proved, that this reaction proceeds by the basic $[SiW_9Nb_3O_{40}]^{7-}$ slowly reacting with trace H_2O to produce OH^-, which in turn yields a slow, OH-induced decomposition of $[SiW_9Nb_3O_{40}]^{7-}$ to produce the required WO_4^{2-}. (b) Lin, Y.; Nomiya, K.; Finke, R. G. *Inorg. Chem.* **1993**, *32*, 6040−6045.

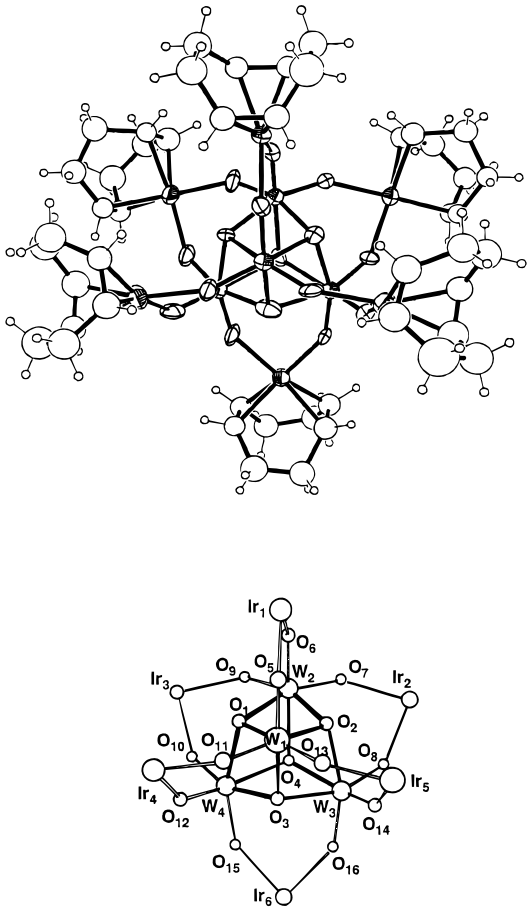

Figure 1. Structure (top) of the anion of **1a**, one of the two independent anions in the asymmetric unit for $2CH_3CN\subset$**1**$\cdot 2CH_3CN$. The two complexed acetonitriles and the two Bu_4N^+ cations associated with **1** have been omitted from this figure for clarity. Cations range of selected distances (Å) and angles (deg): Ir−O, 2.03(2)−2.07(2); Ir−C, 2.03(3)−2.11(3); W−O, 1.78(2)−2.13(2); O−W−O, 73.6(6)−102.8(7); O−Ir−O, 84.0(6)−85.9(5). A ball-and-stick drawing is also provided (bottom) as an aid in visualizing the structure.

terminal oxo ligands per tungsten atom in an *apparent* violation of Lipscomb's rule, which states that there should be no more than two terminal oxo ligands per tungsten atom.[20] However, the binding of the six $[Ir(1,5\text{-COD})]^+$ groups and the resultant stabilization provided by the three O−Ir bonds per tungsten atom means that Lipscomb's rule is in fact not violated. The square-planar geometry about the iridium(I) atoms in **1** is unexceptional,[21] each being coordinated by a 1,5-COD ligand in addition to the two terminal oxygen atoms present over each face of the cubane core. The bridging Ir−O−W angles are in the range 136.6(9)−148.1(9)°.

The mean W−O(bridging) bond length of 2.10(2) Å is ca. 0.10 Å shorter than in the corresponding cubane tetrameric unit in Li_2WO_4.[22] Consideration of bond valence sums for the bridging oxygen atoms makes it clear that they are μ_3-oxo ligands (not μ_3-hydroxo ligands).[23] The topmost iridium atom, Ir1, in Figure 1 sits approximately in the $(W-O)_2-Ir$ plane (deviation from the $(W-O)_2-Ir$ plane is 0.023(8) Å for Ir1 in

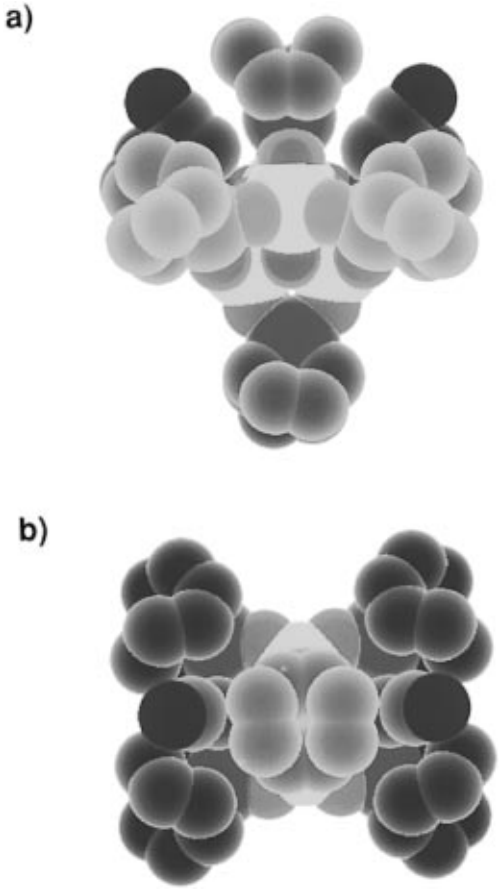

Figure 2. Space filling representation of $2CH_3CN\subset$**1** from (a) the top and (b) the side views (i.e., top and side views relative to the structure provided in Figure 1). Red indicates oxygen, blue nitrogen, green iridium, yellow tungsten, and gray carbon atoms.

1a and 0.176(7) Å for the corresponding atom, Ir10, in **1b**) and has acetonitrile molecules on both sides of that plane. However, the five other $(W-O)_2-Ir$ units, which have an adjacent, included acetonitrile on only one side of the plane, are bent toward the included acetonitrile; as a result, the angles between the IrO_2 and W_2O_2 planes range from 11.6(10)° to 25.0(5)°.

The space-filling view provided in Figure 2 shows that the two included acetonitrile molecules are well buried[24] within the cavities formed by the three surrounding $[Ir(1,5\text{-COD})]^+$ groups (Ir1, Ir2, and Ir5 form one cavity; Ir1, Ir3, and Ir4 form a second cavity). Note that these two occupied cavities sit above two of the four oxygen corners of the W_4O_4 cube and that there are two additional cavities, both of which are unoccupied, formed by $Ir(1,5\text{-COD})^+$ groups above the other two oxygen corners. Figure 3a shows another view looking down on one of the occupied cavities along a pseudo-3-fold axis of the anion of **1**; a similarly oriented view of one of the two unoccupied cavities is shown in Figure 3b. Two $[n\text{-}Bu_4N]^+$ cations are located directly above this second type of cavity but do not sit inside it due to the apparent size mismatch between the cavity and the $[n\text{-}Bu_4N]^+$ ion as well as the shallow nature of this more open cavity. Since there is no specific interaction between the

(20) Lipscomb, W. N. *Inorg. Chem.* **1965**, *4*, 132.

(21) The iridium(I) coordination geometry is similar to that observed in $\{[(1,5\text{-COD})Ir_2\}H(Nb_2W_4O_{19})_2]^{5-}$. Day, V. W.; Klemperer, W. G.; Main, D. J. *Inorg. Chem.* **1990**, *29*, 2345−2355.

(22) Hüllen, A. *Naturwissenschaften* **1964**, *51*, 598−606.

(23) Bond valence sums (according to Brown, I. D.; Altermatt, D. *Acta Crystallogr.* **1985**, *B41*, 244−247) **1a**: W1, 5.92; W2, 5.97; W3, 5.66; W4, 5.68; O1, 2.23; O2, 2.15; O3, 2.22; O4, 2.18. **1b**: W5, 5.92; W6, 5.62; W7, 5.95; W8, 5.72; O17, 2.22; O18, 2.18; O19, 2.18; O20, 2.13.

(24) The acetonitrile methyl carbon atoms are completely buried inside the hydrocarbon environment provided by the three 1,5-COD groups. This is best quantitated by the distances of the acetonitrile C(methyl), C, or N atoms from the least-squares planes defined by the outermost methylene carbon atoms of the three 1,5-COD groups defining the cavity (see Figure 3; + means outside, − means inside the cavity relative to these planes). The range of values which follow are for the four crystallographically independent acetonitrile molecules in the two asymmetric units, **1a** and **1b**: CH_3 (−0.86(3) to −1.08(3) Å), C (+0.31(4) to +0.59(3) Å), N (+1.46(4) to +1.77(3) Å).

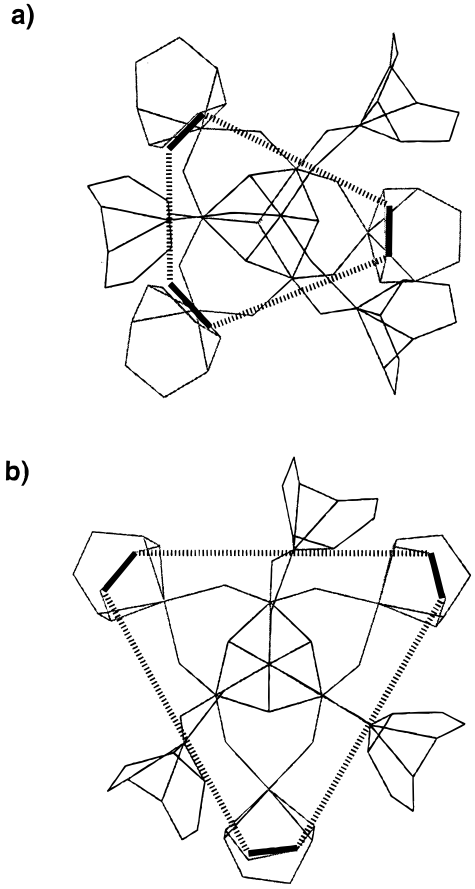

Figure 3. Schematic representation of the *variable size* cavity formed by a group of three of the six total $[Ir(1,5\text{-}COD)]^+$ groups. The distorted hexagon (recognized more readily as an approximate triangle) shows the acetonitrile binding cavity as outlined by the outermost $-CH_2-CH_2-$ methylenes (the three short, thick black lines) of the three 1,5-COD groups. The top figure shows an *acetonitrile binding cavity* approximately along one of the quasi-3-fold axes of the W_4O_4 cubane core, while the bottom figure shows an *open, acetonitrile-free cavity* along a second such axes. This latter cavity is approached, but not occupied, by the Bu_4N^+ cations.

$[n\text{-}Bu_4N]^+$ cations and the anion of **1**, the cations have been omitted from Figures 1−3 for the sake of clarity.

An interesting observation is that, while in the cavity, the *methyl group* of each acetonitrile molecule is oriented toward the cubane core[17,25] and forms weak interactions with the three iridium atoms (C(methyl)···Ir = 3.60(3)-4.02(3) Å), the μ_2-oxygen atoms (C(methyl)···O = 3.10(3)-4.46(4) Å), and the cubane μ_3-oxygen atoms (C(methyl)···O = 3.08(4)-4.02(3) Å). Three novel features of **1** are (a) its organometallic-based cavities (each formed by three adjacent $[Ir(1,5\text{-}COD)]^+$ groups), (b) its flexible size (resulting from the variable $(W-O)_2$-(IrO_2) dihedral angle described above), and (c) its methyl-first CH_3CN binding mode. These three features contrast the rigid, fixed-volume, and all-inorganic cavities described in previous studies[14] and which commonly involve a nitrile-first CH_3CN binding mode.

NMR Studies. In benzene-d_6, the ^1H NMR spectrum of a dissolved crystal of $2CH_3CN\subset\mathbf{1}\cdot 2CH_3CN$ exhibits a single acetonitrile methyl signal at $\delta = 0.62$ indicative of free acetonitrile. Also observed are three broadened *1,5-COD peaks* at $\delta = 1.56$, 2.44, and 4.29, results which require that the Ir-$(1,5\text{-}COD)^+$ bending about the $(W-O)_2-(IrO_2)$ dihedral angle is also time-averaged under these conditions. The ^{183}W NMR of a saturated solution of $2CH_3CN\subset\mathbf{1}\cdot 2CH_3CN$ in $CDCl_3$ confirms the ^1H NMR results by exhibiting the expected single peak at room temperature, which confirms that the $[Ir(1,5\text{-}COD)]^+$ bending about the $(W-O)_2-(IrO_2)$ dihedral angle yields a single, time-averaged geometric isomer.

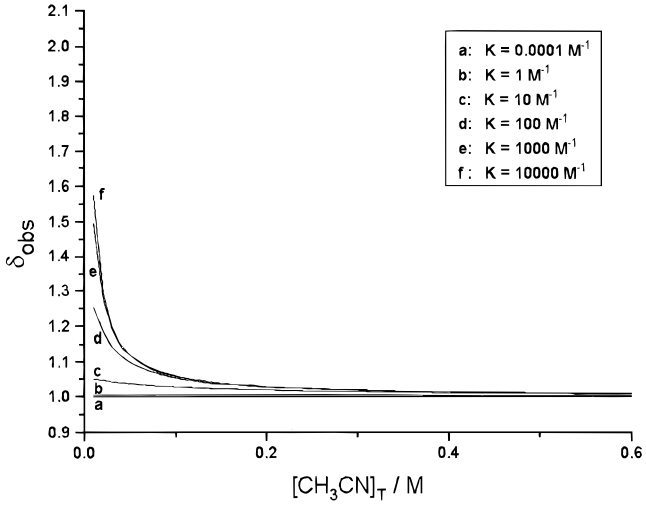

Figure 4. Simulation illustrating the expected δ_{obs} as a function of added $[CH_3CN]$ [calculated for the binding of one CH_3CN and assuming a Δppm difference of 1 ($\delta_{CH_3CN_f} = 1.00$ and $\delta_{\mathbf{1}\cdot CH_3CN} = 2.00$) between free and bound acetonitrile]. [Choosing a larger or smaller Δppm only expands or shrinks the *y* axis but does not change the curve's general shape nor, therefore, the intuitive insights one obtains from this figure.] Note also that δ_{obs} decreases very quickly to the value of free CH_3CN.

^1H NMR studies of acetonitrile-free **1**, synthesized from the solvated complex $2CH_3CN\subset\mathbf{1}\cdot 2CH_3CN$ under vacuum at 50 °C overnight, were carried out to investigate the binding abilities of **1** to guest molecules such as acetonitrile or toluene in solution. However, before beginning any experimental studies, it proved quite useful to obtain an idea of what type of chemical shifts one might expect and what type of binding K_{eq} might be detectable. This proved especially useful in the present case since the methyl-first binding of CH_3CN was expected to be relatively weak, the binding being primarily due to van der Waals and other weak interactions. Simulations of the expected ^1H NMR chemical shift versus $[CH_3CN]_T$ for the situation of CH_3CN binding to **1** are shown in Figure 4.[26] These reveal that a $K_{eq} > 10\ M^{-1}$ is probably required to see a shift in δ_{obs} that is greater than experimental error (and depending upon the

(25) Hayashi, Y.; Ozawa, Y.; Isobe, K. *Inorg. Chem.* **1991**, *30*, 1025−1033. A CH_3CN oriented methyl-first toward a M_6O_{19} core is seen in the polyoxoanion-supported organometallic complex $[(MCp^*)_4V_6O_{19}]\cdot 3CH_3CN\cdot H_2O$ (M = Rh or Ir). However, the CH_3CN is a solid-state-lattice solvate, and not due to inclusion, in this complex which lacks any cavity for true inclusion.

(26) For the simulation of the function of the observed ^1H NMR chemical shift versus $[CH_3CN]_T$ the following equations were used:

$$\delta_{obs} = \delta_{\mathbf{1}\cdot CH_3CN} - \frac{[CH_3CH]_f}{[CH_3CN]_T}(\delta_{\mathbf{1}\cdot CH_3CN} - \delta_{CH_3CN_f}) \qquad (1)$$

$[CH_3CN]_f$ is given by eq 2 (a derivation of eq 2 is provided in the Supporting Information; eq 2 below equals eq 6 therein).

$$[CH_3CN]_f = \{-(K[\mathbf{1}]_T + 1 - K[CH_3CN]_T) + \{(K[\mathbf{1}]_T + 1 - K[CH_3CN]_T)^2 + 4K[CH_3CN]_T\}^{1/2}\}/2K \qquad (2)$$

$$\mathbf{1} + CH_3CN_f \overset{K}{\rightleftharpoons} \mathbf{1}\cdot CH_3CN \qquad (3)$$

where δ_{obs} is the observed ^1H NMR chemical shift, $\delta_{CH_3CN_f}$ is the ^1H NMR chemical shift of free (unbound) CH_3CN, $\delta_{\mathbf{1}\cdot CH_3CN}$ is the ^1H NMR chemical shift of the inclusion complex, **1**, $[CH_3CN]_T$ is the total concentration of CH_3CN, $[CH_3CN]_f$ is the concentration of free (unbound) CH_3CN, and $[\mathbf{1}]_T$ is the total concentration of **1**.

exact Δppm difference between bound and free acetonitrile; Figure 4 is illustrated for a Δppm = 1.0 difference).

Experimentally, a 1.5 mM solution of **1** and a 0.12 M acetonitrile solution were prepared, both in C_6D_6.[27] The desired amount of acetonitrile solution was then injected into the NMR tube containing the solution of **1** using a 10 μL microsyringe (1 mol equiv = 10 μL), and the series of spectra shown in Figure D, Supporting Information, was recorded. In the concentration range from 0 to 20 mM added acetonitrile (0 to 13.4 mol equiv), the ^{1}H NMR signal of acetonitrile does not show any dependence upon the acetonitrile concentration in the presence of 1.5 mM **1**. A control experiment carried out under the exact same conditions, but in the *absence of 1*, gave identical results, confirming that **1** does not bind CH_3CN in solution and under the stated conditions.

Worth recalling at this point is that $2CH_3CN\subset$**1**$\cdot 2CH_3CN$ crystallizes from *neat* acetonitrile. This lead us to explore the highest concentrations of CH_3CN and **1** that we could reasonably obtain experimentally since the acetonitrile complexation is favored under such conditions. A key experimental limitation is that, in benzene and when the $[CH_3CN]_T$ concentration is higher than 20 mM, *the* $2CH_3CN\subset$***1***$\cdot 2CH_3CN$ *inclusion complex precipitates from solution.* (And, as expected, at higher concentrations of **1** (7.6 mM) the inclusion complex starts to precipitate out at much lower CH_3CN concentrations, ca. 2 mol equiv of CH_3CN.) Moreover, NMR examination of a saturated solution of the $2CH_3CN\subset$**1**$\cdot 2CH_3CN$ inclusion complex *in benzene* failed to reveal a signal attributable to bound acetonitrile.

We pushed these solution NMR binding investigations one step further by investigating the NMR of **1** as a function of added CH_3CN, but now in methylene chloride, where the inclusion complex $2CH_3CN\subset$**1**$\cdot 2CH_3CN$ is more soluble. In addition, the 1,5-COD ^{1}H NMR signals rather than the CH_3CN signal were examined so that large concentrations of CH_3CN could be employed. [That is, if bound and free CH_3CN are in fast exchange as one anticipates for weak acetonitrile binding, then the averaged ^{1}H NMR signal for acetonitrile will not be significantly influenced by the (much smaller) signal of bound acetonitrile.] Finally, to avoid overlap of the large CH_3CN signal with the desired 1,5-COD ^{1}H NMR signals of **1**, and to also avoid dynamic range problems when recording the spectra, deuterated acetonitrile (CD_3CN) was used instead of CH_3CN.[28] This series of NMR spectra, titrating a 3 mM solution of **1** in methylene chloride, is shown in Figure E of the Supporting Information. In the concentration range 0−1 M added acetonitrile (0−333 mol equiv), *no discernible shift of the 1,5-COD signals was detected*. (A shift to lower frequency with increasing $[CD_3CN]_T$ is observed for the δ = 3.45 and 1.86 signals of the *n*-Bu_4N^+ groups in **1**, but this is consistent with the expected chemical shift changes arising from solvent effects, especially after 1 M CH_3CN had been added to the CD_2Cl_2 solution.) Last, we also studied toluene as possible guest molecule[29] because of the enhanced chemical shifts expected due to the aromatic ring current, but again, no detectable methyl binding in solution was observed (Figure F, Supporting Information).

Rather clearly, then, the methyl-first binding of CH_3CN is weak as anticipated, probably $K_{eq} < 10\ M^{-1}$. This result is, however, fully consistent with the much larger *nitrile-first* $K_{eq} \approx 150\ M^{-1}$ (at 8 °C in $C_6D_5NO_2$) we calculate from the NMR data reported for $[CH_3CN\subset(V_{12}O_{32}^{4-})]$.[17]

Summary

In conclusion, compound **1** provides the first example of the tetratungstate or $[W_4O_4]^{n+}$ cube structure in a discrete complex of unprecedented composition and structure among polyoxoanion-supported organometallic compounds. This new, hybrid inorganic−organometallic complex with its polyoxoanion foundation yields, in turn, a novel, flexible CH_3CN binding cavity as a result of the fluxionality of the six Ir(1,5-COD)$^+$ groups. This new type of host displays an interesting inclusion chemistry in two ways: (1) inclusion of *neutral guest molecules* in the solid state and (2) an unusual, methyl-first acetonitrile binding motif. NMR studies showed that the binding between **1** and CH_3CN is rather weak as expected, probably $K_{eq} < 10\ M^{-1}$.

An interesting question is whether complex **1** is unique or is just the first member of a family with bound, CH_3-containing molecules such as CH_4, CH_3X, or $CH_3(CH_2)_nX$ (X = OH, halogen, others, and their CD_3-X analogues). One also wonders whether or not photochemically, electrochemically, or thermally induced activation of the CH_3-X methyl hydrogens or X group by the cubane $[W_4O_4]^{n+}$ surface oxygen atoms is possible in this, or a related, complex? Although the weakness of the binding may mitigate against the success of such reaction studies, our intuition is that **1** is just an early member of a larger class of complexes containing substrate guests bound via a novel methyl-first inclusion motif.

Experimental Section

Materials. (*n*-$Bu_4N)_2WO_4$ was prepared according to the published literature procedure.[30] The iridium complex $[Ir(1,5\text{-COD})Cl]_2$ was purchased from Strem Chemicals. Deuterated NMR solvents ($CDCl_3$, CD_2Cl_2, CD_3CN) were used as received apart from C_6D_6, which was dried overnight over molecular sieve (4 Å). All other reagents and materials were obtained from the usual commercial sources and were used as received.

Air- and Moisture-Free Technique. All manipulations were routinely carried out under an inert atmosphere in a Vacuum Atmospheres inert drybox. Dioxygen levels were maintained at less than 1.0 ppm as monitored by use of a Vacuum Atmospheres O_2 monitor. The inclusion compound tended to lose nonincluded solvent molecules when exposed to the atmosphere and also proved to be hygroscopic.

Instruments. NMR spectra were recorded on a Bruker AC 300 P spectrometer operating at 300.15 (^{1}H) and 75.0 MHz (^{13}C) or a Bruker AM 500 operating at 15.04 MHz (^{183}W). Chemical shifts were referenced to the residue proton signal of the deuterated solvents (C_6D_6, δ = 7.16; CD_2Cl_2, δ = 5.32; $CDCl_3$, δ = 7.27) or the ^{13}C NMR signal of the solvent ($CDCl_3$, δ = 77.23) or 2 M Na_2WO_4/D_2O (^{183}W, pD 8.0, external reference by the substitution method) and are reported on

(27) Special care has to be taken when working with **1** in low concentrations since the signals of common impurities were observed to show up in the ^{1}H NMR spectra in similar intensity to the complex signals at chemical shifts in the range seen for authentic CH_3CN (e.g., in C_6D_6: H_2O, $\delta \approx 0.4$; Dow Corning high vacuum grease, $\delta \approx 0.3$). The low solubility of $2CH_3CN\subset$**1**$\cdot 2CH_3CN$ and, therefore, its tendency to precipitate from solution when formed (i.e., when sufficient CH_3CN is present) is another property that can give rise to experimental artifacts if not avoided (e.g., see Figure G of the Supporting Information).

(28) This experiment assumes that the anticipated slightly smaller size of the CD_3 group in comparison to a CH_3 group does not effect significantly the acetonitrile binding constant. This assumption was confirmed by using CH_3CN instead of CD_3CN under the exactly same conditions and showing that the experiment with protio-CH_3CN gave results identical (i.e., for the nonoverlapping sections of the ^{1}H NMR spectrum) to those observed with CD_3CN.

(29) We considered using *N*-methylpyridinium salts as guest compounds which should bind to the $[\{Ir(1,5\text{-COD})\}_6W_4O_{16}]^{2-}$ dianion more tightly because of Coulombic attractions. However, since pyridinium salts might replace the *n*-Bu_4N^+ groups in the complex (i.e., bind at the sites where the *n*-Bu_4N^+ groups are located rather than at the Me-binding site), this potential experiment was abandoned.

(30) (*n*-$Bu_4N)_2[WO_4]$ was prepared according to the literature procedure in: Che, T. M.; Day, V. W.; Francesconi, L. C.; Fredrich, M. F.; Klemperer, W. G.; Shum, W. *Inorg. Chem.* **1985**, *24*, 4055−4062.

the δ scale. Infrared spectra were recorded as Nujol mulls on NaCl plates using a Nicolet 5DX spectrophotometer. Mass spectra were obtained using fast-atom-bombardment and a *m*-nitrobenzyl alcohol matrix. Microanalyses were performed by Mikroanalytisches Labor Pascher (Remagen, Germany).

$2CH_3CN\subset(n\text{-}Bu_4N)_2[\{Ir(1,5\text{-}COD)\}_6W_4O_{16}]\cdot 2CH_3CN$ ($2CH_3CN\subset$1$\cdot 2CH_3CN$). $(n\text{-}Bu_4N)_2WO_4$ (426 mg, 0.58 mmol) and $[Ir(1,5\text{-}COD)Cl]_2$ (518 mg, 0.77 mmol) were dissolved in acetonitrile (10 mL) with stirring in a Vacuum Atmospheres drybox. The solution was heated at 50 °C for 30 min, after which a trace amount of undissolved material was removed by filtration resulting in a clear solution. After reducing the volume of the solution to 4 mL under reduced pressure, the homogeneous light-brown solution was allowed to cool to room temperature. Pale-yellow, crystalline, air-sensitive $2CH_3CN\subset$1$\cdot 2CH_3CN$ formed slowly, after ca. one-half day. Yield: 641 mg (73% based on $[Ir(1,5\text{-}COD)Cl]_2$). Recrystallization from room-temperature acetonitrile over 3−4 days afforded light-yellow single crystals suitable for X-ray crystallography. Crystals of $2CH_3CN\subset$1$\cdot 2CH_3CN$ immediately lose acetonitrile and become opaque when removed from the mother liquor, a property which precluded obtaining a precise, all-elements elemental analysis even if the crystals were transported in a sealed ampule. For NMR investigations, the crystals were collected in a 15-mL medium frit, sintered glass filter funnel, thoroughly dried with aspiration (15 min), and then allowed to dry further for 1 h on the frit, all in the drybox. For $C_{80}H_{144}N_2Ir_6O_{16}W_4\cdot 4CH_3CN$ (3446), calcd: C, 30.70; H, 4.57; N, 2.44; O, 7.44; Ir, 33.50; W, 21.36; total, 100.0. Found: C, 29.64; H, 4.54; N, 2.31; O, 7.82; Ir, 33.5; W, 21.4; total, 99.21. ^{1}H NMR (300 MHz, C_6D_6, 25 °C): δ = 4.29 (b, 24 H, (COD)CH═), 3.59 (b, 16 H, $BuCH_2$), 2.44 (b, 24 H, (COD)CH_2−), 1.86 (b, 16 H, $BuCH_2$), 1.56 (q, 24 H, (COD)CH_2−), 1.46 (q, 16 H, $BuCH_2$), 0.86 (t, 24 H, $BuCH_3$), 0.67 (12 H, CH_3CN). ^{1}H NMR (300 MHz, $CDCl_3$, 25 °C): δ = 3.77 (b, 16 + 24 H, $BuCH_2$ + (COD)CH═), 2.26 (b, 24 H, (COD)CH_2−), 2.11 (b, 16 H, $BuCH_2$), 2.06 (12 H, CH_3CN), 1.62 (q, 16 H, $BuCH_2$), 1.36 (q, 24 H, (COD)CH_2−), 1.09-(t, 24 H, Bu-CH_3). ^{13}C NMR (300 MHz, $CDCl_3$, 25 °C): δ = 60.7, 55.2, 32.1, 25.7, 20.7, 14.0. ^{183}W NMR (500 MHz, $CDCl_3$, 25 °C, Na_2WO_4): δ = 72.3 ppm. IR (Nujol): ν = 835 cm^{-1} (W−O and Ir−O). FAB MS (3-nitrobenzyl alcohol matrix): *m*/*z* 3278 $[M]^+$, 3038 $[M - (n\text{-}Bu_4N) + 2H]^+$.

Nonsolvated $(n\text{-}Bu_4N)_2[\{Ir(1,5\text{-}COD)\}_6W_4O_{16}]$ (1). Nonsolvated, acetonitrile-free **1** was prepared from $2CH_3CN\subset$1$\cdot 2CH_3CN$ by desolvation under vacuum (ca. 0.01 Torr) at 50 °C overnight (24 h total). The NMR data are identical with the $2CH_3CN\subset$1$\cdot 2CH_3CN$ data with the exception of the additional CH_3CN signal (δ = 0.67 in C_6D_6 and δ = 2.06 in $CDCl_3$) in the case of $2CH_3CN\subset$1$\cdot 2CH_3CN$. In the case of acetonitrile-free **1**, a satisfactory, all-elements elemental analysis was possible. For $C_{80}H_{144}N_2Ir_6O_{16}W_4$ (3278), calcd: C, 29.30; H, 4.43; N, 0.85; O, 7.81; Ir, 35.18; W, 22.39; total, 100.0. Found: C, 29.00; H, 4.46; N, 1.20; O, 8.50; Ir, 34.7; W, 22.2; total, 100.0.

X-ray Diffraction Study of $2CH_3CN\subset$1$\bullet 2CH_3CN$. A single crystal (see Table 1 for crystallographic data) was sealed under nitrogen in a thin-walled glass capillary along with a minimum amount of mother liquor (sufficient only to coat the inside of the capillary). X-ray diffraction data were recorded on a Siemens SMART CCD diffractometer employing Mo Kα radiation (graphite monochromator). The cell parameters listed were obtained from a least-squares fit to the angular coordinates of 148 reflections on a series of oscillation frames. For the entire data set (θ = 1.36−23.22°), limiting indices were $-19 \leqslant h \leqslant 27$, $-13 \leqslant k \leqslant 20$, $-50 \leqslant l \leqslant 32$. Intensities were integrated from a series of frames (0.3° ω rotation) covering more than a hemisphere of reciprocal space. Absorption and other corrections were applied by using SADABS[31] (transmission factors 0.089−0.033; R_{int} improved from 0.1785 to 0.037). A total of 42 659 measured reflections were merged to provide a data set comprised of 27 451 unique reflections (R_{int} = 0.05), 27 435 of which would be "observed" on the basis of the criterion $F_o^2 > 2\sigma(F_o^2)$.

The structure was solved by direct methods and refined (on F,^{2} using all data) by a full-matrix, weighted ($w^{-1} = \sigma^2(F_o^2) + (0.0474P)^2 + 484.34P$, where $P = (F_o^2 + 2F_c^2)/3$) least-squares process. Standard Siemens control (SMART) and integration (SAINT) software was employed, and SIEMENS SHELXTL[32] software was used for structure solution, refinement, and graphics. All heavy atoms and oxygen atoms were refined with anisotropic displacement parameters, and all carbon and nitrogen atoms were refined with isotropic displacement parameters. The residual electron density within 1.0 Å of Ir4 was initially greater than 10 e Å^{-3}; this was interpreted as being due to disorder of the $Ir(1,5\text{-}COD)^+$ group to the other side of the W_2O_2 plane (subsequent refinement of the site occupancy factor for Ir4 converged at 82%). For Ir4′ (18% occupancy factor) only three carbon atoms of the coordinated 1,5-COD group could be located in the difference Fourier map; hence, this minority 1,5-COD ligand was modeled by transposing the 1,5-COD ligand bound to Ir4 and constraining its metric parameters to be similar to those of the majority ligand. The other iridium atoms did not exhibit clear disorder, but generally exhibited relatively large residual electron density (maximum 3.8 e Å^{-3}) at the end of the refinement.[33] The n-Bu_4N^+ cations containing N3 and N4 exhibited disorder involving the hydrocarbon chains that was so severe that some of the atoms could not be identified. In one of the chains attached to N4, the N−C and C−C bond distances had to be constrained during refinement. Hydrogen atoms were not placed on the disordered moieties; all other hydrogen atoms were fixed in idealized positions. The isotropic displacement parameters for acetonitrile hydrogen atoms were fixed (U_{iso} = 0.1). Refinement was taken to convergence (maximum shift/esd = 0.147, mean shift/esd = 0.005 on the last cycle) for this model. The final difference electron density map showed features in the range +3.8 to −2.5 e Å^{-3}, with the highest peak being 1.05 Å from Ir9.

Table 1. Crystal Data and Structure Refinement for $2CH_3CN\subset(n\text{-}Bu_4N)_2[\{Ir(1,5\text{-}COD)\}_6W_4O_{16}]\cdot 2CH_3CN$ ($2CH_3CN\subset$1$\cdot 2CH_3CN$)

empirical formula	$C_{88}H_{156}Ir_6N_6O_{16}W_4$
formula weight	3442.8
temperature, K	159(2)
wavelength, Å	0.710 73
space group	$P2_1/n$
unit cell dimens	
a, Å	24.8856(6)
b, Å	18.6662(5)
c, Å	45.7427(12)
β, deg	93.5450(10)
V, Å^3	21 207.7(9)
Z	8
density (calcd), g cm^{-3}	2.157
absorption coeff, mm^{-1}	11.873
F(000)	12 896
crystal size, mm	0.40 × 0.20 × 0.15
no. of reflns colld	42 659
no. of independent reflns	27451 [*R*(int) = 0.0500]
no. of data/restraints/params	27 435/61/1263
goodness-of-fit on F^2	1.048
final *R* indices [$I > 2\sigma(I)$][a]	R_1 = 0.0655, wR_2 = 0.1340
R indices (all data)	R_1 = 0.1197, wR_2 = 0.1811
max diff. peak; hole, e Å^{-3}	3.831; −2.484

[a] $R_1 = [\sum(|F_o| - |F_c|)]/[\sum|F_o|]$; $wR_2 = [[\sum w(F_o^2 - F_c^2)^2]/[\sum w(F_o^2)^2]]^{1/2}$.

NMR Inclusion Studies of 1 Plus CH_3CN in C_6D_6, [1] = 1.5 mM. In a drybox, 5 mg of **1** was weighed into a 1 mL volumetric flask which was filled with 1 mL of C_6D_6 to yield a 1.5 mM solution. After all **1** had dissolved, this solution was transferred into a 5 mL glass vial and 0.8 mL of this solution was transferred into an NMR tube using a 1 mL Eppendorf pipet. The NMR tube was closed with a septum cap and sealed with parafilm. Next, 5 mg of CH_3CN was weighed into another 1 mL volumetric flask which was filled with 1 mL of C_6D_6 to yield a 0.12 M solution, closed with a septum cap, and sealed with

(31) Sheldrick, G. M. SADABS—a program for area detector absorption corrections, private communication.

(32) Sheldrick, G. M. *SHELXTL, v. 5.03*; Siemens Analytical X-ray Instruments: Madison, WI, 1995.

(33) A listing of, and references to, the well-known difficulties in polyoxoanion structure determination and refinement (e.g., disorder, ghost electron density near heavy atoms, inability to locate organic ligands or counterions, etc.) are available in footnote 13 of the following reference: Weakley, T. J. R.; Finke, R. G. *Inorg. Chem.* **1990**, *29*, 1235−1241.

parafilm. The desired amount of CH_3CN solution was then injected into the NMR tube containing the solution of **1** using a 10 μL microsyringe (1 mol equiv = 10 μL). Both solutions were always freshly prepared prior to recording a series of NMR experiments.

NMR Control Experiment: Concentration Dependence of the ^{1}H NMR CH_3CN Signal in the Absence of 1. To start, 0.8 mL of C_6D_6 was transferred into an NMR tube using an Eppendorf pipet. The NMR tube was closed with a septum cap and sealed with parafilm. Next, 5 mg of CH_3CN was weighed into a 1 mL volumetric flask which was filled with C_6D_6 to yield a 0.12 M solution, closed with a septum cap, and sealed with parafilm. The desired amount of 0.12 M CH_3CN solution was then injected into the NMR tube containing C_6D_6 using a 10 μL microsyringe.

NMR Contol Experiment: ^{1}H NMR spectrum of a saturated solution of 1 plus CH_3CN. In a drybox, 40 mg of CH_3CN was dissolved in 1 mL of C_6D_6. This solution was then added to 5 mg of **1**. The solution was heated to 50 °C for 1 h, filtered (not all of the material dissolves), and then investigated by ^{1}H NMR spectroscopy.

NMR Inclusion Studies of 1 plus CH_3CN in CD_2Cl_2, $[CH_3CN]_T \leqslant$ 1 M. In a drybox 10 mg of **1** was weighed into a 1 mL volumetric flask which was filled with 1 mL of CD_2Cl_2 to yield a 3 mM solution. After all **1** had dissolved, this solution was transferred into a 5 mL glass vial and 0.8 mL of this solution transferred into an NMR tube using an 1 mL Eppendorf pipet. The NMR tube was closed with a septum cap and sealed with parafilm. The desired amount of neat CH_3CN or CD_3CN, respectively, was then injected into the NMR tube containing the solution of **1** using a 10 μL microsyringe (1 μL $\approx$ 6.3 mol equiv).

NMR Inclusion Studies of 1 Plus Toluene in CD_2Cl_2. In a drybox 10 mg of **1** was weighed into a 1 mL volumetric flask which was filled with 1 mL of CD_2Cl_2 to yield a 3 mM solution. After all **1** had dissolved, this solution was transferred into a 5 mL glass vial and 0.8 mL of this solution transferred into an NMR tube using an 1 mL Eppendorf pipet. The NMR tube was closed with a septum cap and sealed with parafilm. Next, 22 mg of toluene was weighed into another 1 mL volumetric flask which was filled with 1 mL of CD_2Cl_2 to yield a 0.24 M solution. The flask was closed with a septum cap and sealed with parafilm. The desired amount of the 0.24 M toluene solution or neat toluene-d_8, respectively, was then injected into the NMR tube containing **1** using a 10 μL microsyringe (0.24 M solution: 1 mol equiv $\approx$ 5 μL; neat toluene-d_8: 1 μL $\approx$ 3.8 mol equiv). For the NMR spectra at 0.5, 1, 2, and 11 mol equiv, the 0.24 M toluene solution was used. For the spectra at 44, 144, and 344 mol equiv, neat CD_3CN was used.

Acknowledgment. Financial support was provided by NSF Grant CHE 9531110. The Siemens SMART CCD X-ray diffraction system was provided by the NIH (Grant No. RRO-10547).

Supporting Information Available: Crystallographic summary for $2CH_3CN\subset$**1**$\cdot 2CH_3CN$ including tables of crystal data, atomic coordinates and equivalent isotropic displacement parameters, selected interatomic distances, bond lengths and angles, anisotropic displacement parameters, hydrogen atom coordinates, and isotropic displacement parameters; Figure A, molecular structure of $2CH_3CN\subset$**1**$\cdot 2CH_3CN$ including the two acetonitrile and two n-Bu_4N^+ cations; Figure B, FAB mass spectra of $2CH_3CN\subset$**1**$\cdot 2CH_3CN$; Figure C, ^{1}H NMR spectrum of **1** in benzene-d_6 plus signal assignments; Figure D, ^{1}H NMR spectra showing the acetonitrile signal in presence of 1.5 mM **1** with increasing $[CH_3CN]_T$; Figure E, ^{1}H NMR spectra of 3 mM **1** with increasing $[CD_3CN]_T$ in CD_2Cl_2; Figure F, ^{1}H NMR spectra of 3 mM **1** with increasing $[\text{toluene}]_T$ in CD_2Cl_2; Figure G, observed δ_{CH_3CN} versus added $[CH_3CN]_T$ that illustrates the artifactual curve one sees if the precipitation of $2CH_3CN\subset$**1**$\cdot 2CH_3CN$ occurs; derivation of eq 2 (33 pages). See any current masthead page for ordering and Internet access instructions.

JA970336H